Visual Abstract

The impact of the temperature and exploitation time on the tensile properties and plain strain fracture toughness, K_{Ic} in characteristic areas of welded joint

Ivica Čamagić
Faculty of Technical Sciences, Kosovska Mitrovica, Serbia
Ivica.camagic@pr.ac.rs

Simon A. Sedmak
Innovation Centre of Faculty of Mechanical Engineering, Belgrade, Serbia
Simon.sedmak@yahoo.com

Aleksandar Sedmak
Faculty of Mechanical Engineering, University of Belgrade, Serbia
asedmak@mas.bg.ac.rs

Zijah Burzić
Military Technical Institute, Belgrade, Serbia
Zijah.burzic@gmail.com

Mihajlo Aranđelović
Innovation Centre of Faculty of Mechanical Engineering, Belgrade, Serbia
Mixaylo23@gmail.com

ABSTRACT. This paper presents the analysis of the temperature and exploitation time impact on the resistant measure to brittle fracture of welded joint constituents of the new and exploited low-alloyed Cr-Mo steel A-387 Gr. B from the aspect of application of the parameters obtained by tensile testing and parameters obtained by fracture mechanics testing. The exploited parent metal is a part of the reactor mantle which has working for over 40 years and is in the damage repair stage, wherein it is being replaced with a new material. Basic characteristics of the material strength, as well as the stress-elongation curves required for stress analysis are obtained by tensile testing. The testing of plane strain fracture toughness is conducted in order to determine the critical stress intensity factor, K_{Ic}, that is, assessment of behavior of the new and exploited parent metal, welded metal and heat affected zone from the side of the new parent metal and from the side of the exploited parent metal in the

Citation: Čamagić, I, Sedmak, S. A., Sedmak, A., Burzić, Z., Aranđelović, M., The impact of the temperature and exploitation time on the tensile properties and plain strain fracture toughness, KIc in characteristic areas of welded joint , Frattura ed Integrità Strutturale, 46 (2018) 371-382.

Received: 05.08.2018
Accepted: 21.09.2018
Published: 01.10.2018

presence of the crack type error. Based on the research results, the analysis of the resistance to brittle fracture was performed in order to compare the obtained values for characteristic areas of welded joint and justify the selection of welding technology.

KEYWORDS. Welded joint; Tensile properties; Plane strain fracture toughness; Critical crack length.

INTRODUCTION

A long-time exploitation period of a pressure vessel-reactor (over 40 years) has caused certain damages to the reactor mantle. The occurrence of these damages required a thorough inspection of the reactor construction itself, as well as the repair of damaged parts. Repairing of the reactor included the replacement of a part of the reactor mantle with newly built-in material. The given pressure vessel was made of low-alloyed Cr-Mo steel A-387 Gr. B in accordance with ASTM standard with (0.8-1.15)% Cr and (0.45-0.6)% Mo. For designed working parameters (p = 35 bar and t = 537°C) the material is in the area of tendency towards decarbonisation of the surface which is in contact with hydrogen. The surface decarbonisation may reduce the strength of the material. The reactor, based on its construction represents a vertical pressure vessel with a cylindrical mantle. Deep lids of the same quality as the reactor mantle are welded to upper and lower side of the mantle. The most important process in motor gasoline production stage takes place in the reactor- a platforming for altering the structure of hydrocarbon compounds and achieving a higher gasoline octane number. Testing of a new and exploited parent metal (PM), the weld metal-WM and heat affected zone (HAZ), included the determinating of tensile properties and fracture mechanics parameters of the new and exploited PM and welded joint components (WM and HAZ), at room and working temperature of 540°C, [1].

Welding technology qualification for sheets made of new and exploited PM was performed in accordance with standard SRPS EN ISO 15614-1, [2]. The research performed here was based on the experiences from previous experiments involving the determining of fracture toughness and fatigue crack growth parameters at room and working temperatures, as seen in [3,4].

MATERIALS FOR TESTING

Both exploited (E) and new (N) steel A-387 Gr. B with thickness of 102 mm were analyzed. Chemical composition and mechanical properties of the exploited and new PM according to the attest documentation are given in Tab. 1 and 2, [1]. Welding of steel sheets made of exploited and new PM was performed in two stages, according to the requirements given in the welding procedure provided by a welding specialist, and these stages include:

- Root weld by E procedure, using a coated LINCOLN S1 19G electrode (AWS: E8018-B2), and
- Filling by arc welding under powder protection (EPP), where wire denoted as LINCOLN LNS 150 and powder denoted as LINCOLN P230 were used as additional materials.

Chemical composition of the coated electrode LINCOLN S1 19G, and the wire LINCOLN LNS 150 according to the attest documentation is given in Tab. 3, whereas their mechanical properties, also according to the attest documentation, are given in Tab. 4, [1].

Specimen mark	% max.							
	C	Si	Mn	P	S	Cr	Mo	Cu
E (Exploited)	0.15	0.31	0.56	0.007	0.006	0.89	0.47	0.027
N (new)	0.13	0.23	0.46	0.009	0.006	0.85	0.51	0.035

Table 1: Chemical composition of exploited and new PM specimens.

Specimen mark	Yield stress, $R_{p0.2}$, MPa	Tensile strength, R_m, MPa	Elongation, A, %	Impact energy, J
E	320	450	34.0	155
N	325	495	35.0	165

Table 2: Mechanical properties of exploited and new PM specimens.

Additional material	% max.						
	C	Si	Mn	P	S	Cr	Mo
LINCOLN Sl 19G	0.07	0.31	0.62	0.009	0.010	1.17	0.54
LINCOLN LNS 150	0.10	0.14	0.71	0.010	0.010	1.12	0.48

Table 3: Chemical composition of additional welding materials.

Additional material	Yield stress, $R_{p0.2}$, MPa	Tensile strength, R_m, MPa	Elongation, A, %	Impact energy, J at 20°C
LINCOLN Sl 19G	515	610	20	> 60
LINCOLN LNS 150	495	605	21	> 80

Table 4: Mechanical properties of filler materials.

DETERMINATION OF TENSILE PROPERTIES

Basic characteristics of material strength, as well as the stress-elongation curves required for stress analysis, are obtained by tensile testing. Tensile testing of butt welded joint at room temperature, including the shape and dimensions of specimens as well as the procedure itself are defined by SRPS EN 895:2008 standard, [5]. This standard primarily defines transverse tension, i.e. introduction of the load transversely to the welded joint.
SRPS EN 895:2008 standard also envisages the determination of the tensile properties of PM and WM at room temperature. Determination of tensile properties of PM is defined by SRPS EN 10002-1 standard, [6].

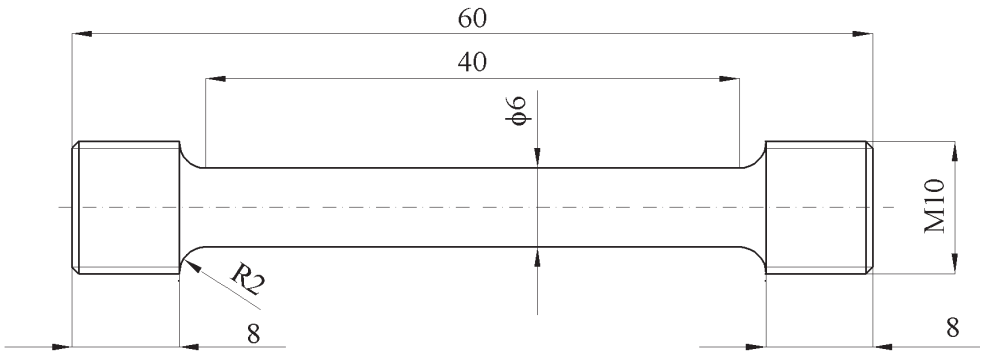

Figure 1: Tensile test specimens for WM and HAZ.

Unlike room temperature testing, the testing procedures at increased temperature of 540°C, as well as the specimen geometry are defined by SRPS EN 10002-5 standard, [7]. The specimens used for determining of tensile properties of WM and HAZ, as well as for working temperature tensile tests are shown in Figs. 1 and 2, respectively.

Testing results of butt welded joint specimens by transverse tension at room temperature of 20°C and working temperature of 540°C are given in Tab. 5, [1]. Typical tensile stress-elongation curve for specimen of butt welded joint marked as WJ-1-1, tested at room temperature is shown in Fig. 3, left [1], and for specimen marked as WJ-2-1, tested at working temperature is shown in Fig. 3, right.

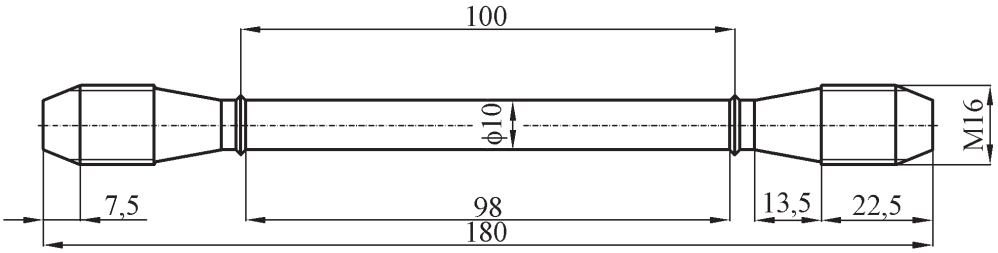

Figure 2: Specimens for tensile testing at working temperature.

Specimen designation	Testing temperature, °C	Yield stress, $R_{p0.2}$, MPa	Tensile strength, R_m, MPa	Elongation1, A, %	Fracture location
WJ-1-1		295	451	19.2	Expl. PM
WJ-1-2	20	285	448	20.4	Expl. PM
WJ-1-3		291	454	19.7	Expl. PM
WJ-2-1		217	293	26.3	Expl. PM
WJ-2-2	540	205	285	25.6	Expl. PM
WJ-2-3		211	287	26.9	Expl. PM

[1] measured at L_0 = 100mm, as comparative value (not as a material property).

Table 5: Results of tensile testing of the welded joint.

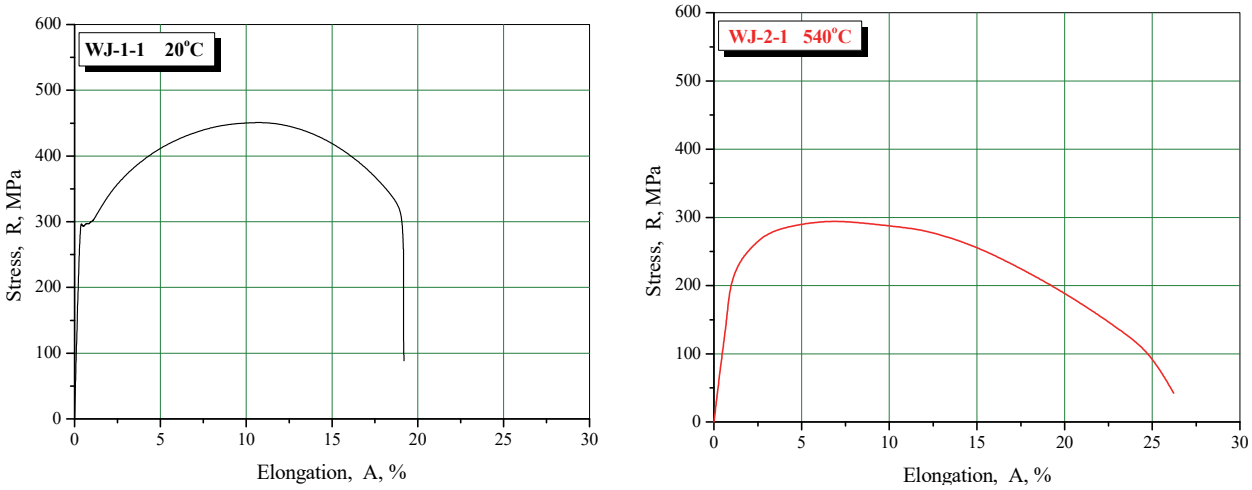

Figure 3: Stress-elongation diagram of a butt welded joint specimen WJ-1-1 (left) and specimen WJ-2-1 (right).

Testing results of specimens of the new PM at room temperature of 20°C and working temperature 540°C are given in Tab. 6, [1]. Testing of exploited PM was not performed, because during the testing of welded joint specimens all tested specimens fractured in the exploited PM, which provided us with the properties of exploited PM. typical tensile stress-elongation curve for specimen denoted by PM-1-1N, taken from the new PM and tested at room temperature is given in Fig. 4, left [1], and for specimen PM-2-1N, also taken from the new PM, but tested at working temperature, is shown in Fig. 4, right [1].

Specimen designation	Testing temperature. °C	Yield stress. Rp0.2. MPa	Tensile stress. Rm. MPa	Elongation. A. %
PM-1-1N	20	342	513	27.5
PM-1-2N		339	505	28.3
PM-1-3N		335	498	28.6
PM-2-1N	540	251	323	29.1
PM-2-2N		242	316	30.8
PM-2-3N		247	320	30.4

Table 6: Results of tensile testing of new PM specimens.

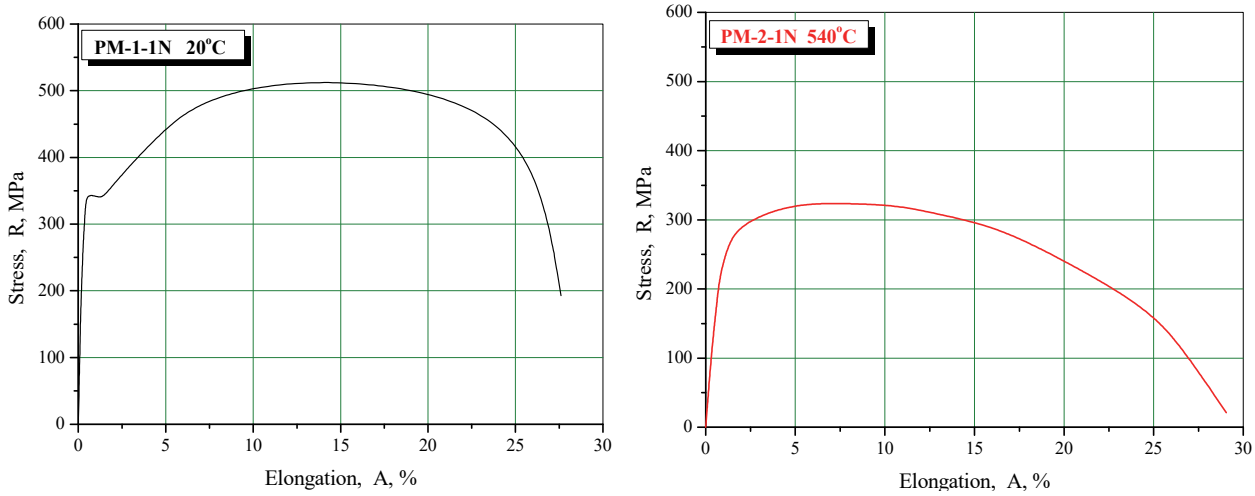

Figure 4: Stress-elongation diagram of a new PM specimen PM-1-1N (left) and new specimen PM-2-1N (right).

Testing results of WM specimens tested at room temperature of 20°C and working temperature of 540°C are given in Tab. 7, [1]. Typical tensile stress-elongation curve for WM specimen marked as WM-1-1, tested at room temperature is shown in Fig.5, left [1], and for specimen marked as WM-2-1, tested at working temperature is shown in Fig. 5, right [1].

Specimen designation	Testing temperature, °C	Yield stress, $R_{p0.2}$, MPa	Tensile strength, R_m, MPa	Elongation, A, %
WM-1-1	20	518	611	20.9
WM-1-2		510	597	22.7
WM-1-3		514	605	21.3
WM-2-1	540	331	419	26.1
WM-2-2		319	406	27.3
WM-2-3		325	412	27.7

Table 7: Results of tensile testing of WM specimens.

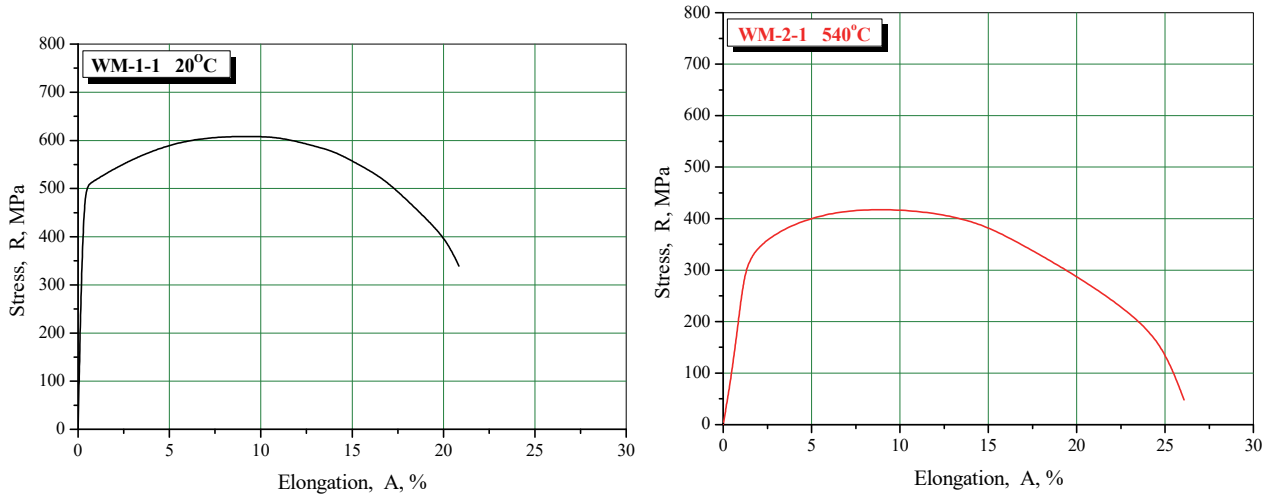

Figure 5: Stress-elongation diagram for WM specimen, WM-1-1 (left) and WM specimen WM-2-1 (right)

DETERMINATION OF PLANE STRAIN FRACTURE TOUGHNESS, K_{Ic}

The impact of exploitation conditions, i.e. exploitation time and temperature on tendency to brittle fracture of the new and exploited PM, as well as the components of welded joint (WM and HAZ) was evaluated by determining the plane strain fracture toughness, that is, critical value of stress intensity factor, K_{Ic}. The testing was performed at room temperature of 20°C and working temperature of 540°C.

For determination of, K_{Ic}, at room temperature the three point bending specimen (SEB) were used, whose geometry is defined by ASTM E399, [8], and ASTM E1820 standards, [9]. For determination of K_{Ic} at working temperature of 540°C the modified CT tensile specimens were used, whose geometry is in accordance with BS 7448 Part 1, standard, [10].

Fracture toughness, K_{Ic}, is determined indirectly through critical J-integral, J_{Ic}, using elastic-plastic fracture mechanics (EPFM) defined by ASTM E813, [11], ASTM E 1737, [12], ASTM E1820, [9] and BS 7448 Part 1 and 2, [10, 13] standards, that is, by monitoring the crack development in the conditions of plasticity.

The American society for testing and materials (ASTM) has established a standard procedure for obtaining the crack growth resistance curves of metallic materials, [12]. The improvement of the standard was carried out within the framework of the European Structural Integrity Society ESIS, [14]. Some of the solutions of this standard are also adopted in this paper and refer to the determination of fitted regression line. Standards, [8, 9, 11, 12, 15-17], regularly updates, and it is very important to make sure that the latest versions are applied.

The experiments are carried out by the testing method of a single specimen by successive partial unload, i.e. by the single specimen permeability method, as defined by ASTM E813, standard, [11].

Based on the obtained data, J-Δa curve is constructed on which the regression line is constructed according to ASTM E1152, [16]. From the obtained regression line the critical J-integral, J_{Ic}, is obtained. Knowing the value of critical, J_{Ic}, integral, the value of critical stress intensity factor or plane strain fracture toughness, K_{Ic}, can be calculated using the dependence:

$$K_{Ic} = \sqrt{\frac{J_{Ic} \cdot E}{1-\upsilon^2}} \tag{1}$$

Calculated values of critical stress intensity factor, K_{Ic}, are given in tab. 8 for notched specimens in new PM, and in tab. 9 for notched specimens in exploited PM, tested at room temperature of 20°C and working temperature of 540°C, [1].

It is important to point out that in calculation of plane strain fracture toughness, K_{Ic}, one value was used for elastic modulus at room temperature (210GPa) and other value for increased temperatures (approximately 160GPa for 5400C). By applying basic formula of fracture mechanics:

$$K_{Ic} = \sigma \cdot \sqrt{\pi \cdot a_c} \tag{2}$$

and by introducing the values of conventional yield stress, $R_{p0,2} = \sigma$, [1, 17], the approximate values for critical crack length, a_c, can be calculated.

Specimen mark	Testing temperature. °C	Critical J-integral. J_{Ic}, kJ/m²	Critical stress intensity factor, K_{Ic}, MPa m$^{1/2}$	Critical crack length, a_c, mm
PM-1-1n		60.1	117.8	38.5
PM-1-2n	20	63.9	121.4	40.8
PM-1-3n		58.6	116.3	37.5
PM-2-1n		43.2	87.2	40.0
PM-2-2n	540	44.7	88.7	41.4
PM-2-3n		45.3	89.2	41.9

Table 8: Values of K_{Ic} notched specimens in new PM.

Specimen mark	Testing temperature, °C	Critical J-integral, J_{Ic}, kJ/m²	Critical stress intensity factor, K_{Ic}, MPa m$^{1/2}$	Critical crack length, a_c, mm
PM-1-1e		47.8	105.0	41.7
PM-1-2e	20	42.1	98.6	36.8
PM-1-3e		40.7	96.9	35.6
PM-2-1e		24.5	65.6	30.8
PM-2-2e	540	22.7	63.2	28.6
PM-2-3e		21.8	61.9	27.4

Table 9: Values of K_{Ic} notched specimens in exploited PM.

The characteristic diagrams F-δ, and J-Δa for specimen taken out from the sample of new PM are given in Fig. 6 (left) for specimen marked as PM-1-1n tested at room temperature, and in Fig. 7 for specimen marked as PM-2-1n tested at the temperature of 540°C, [1].

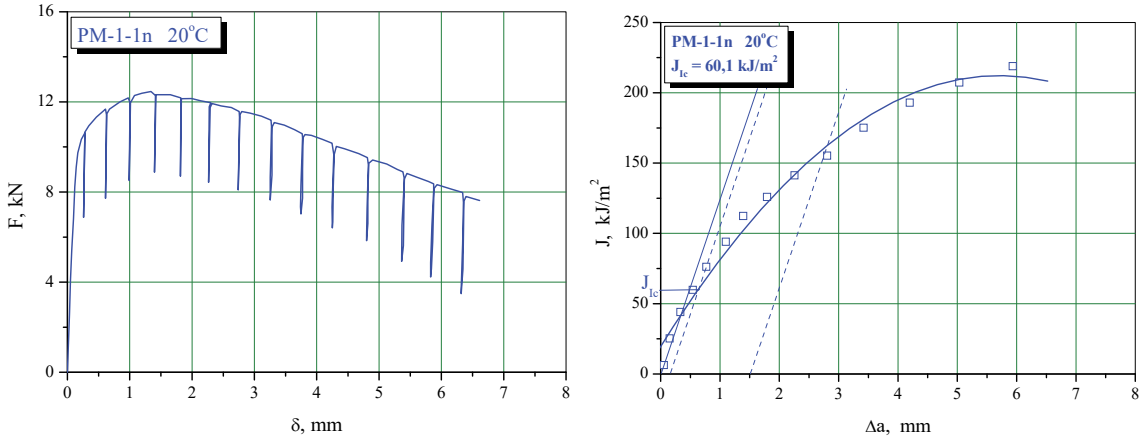

Figure 6: F-δ (left) and J-Δa (right) diagrams of specimen PM-1-1n.

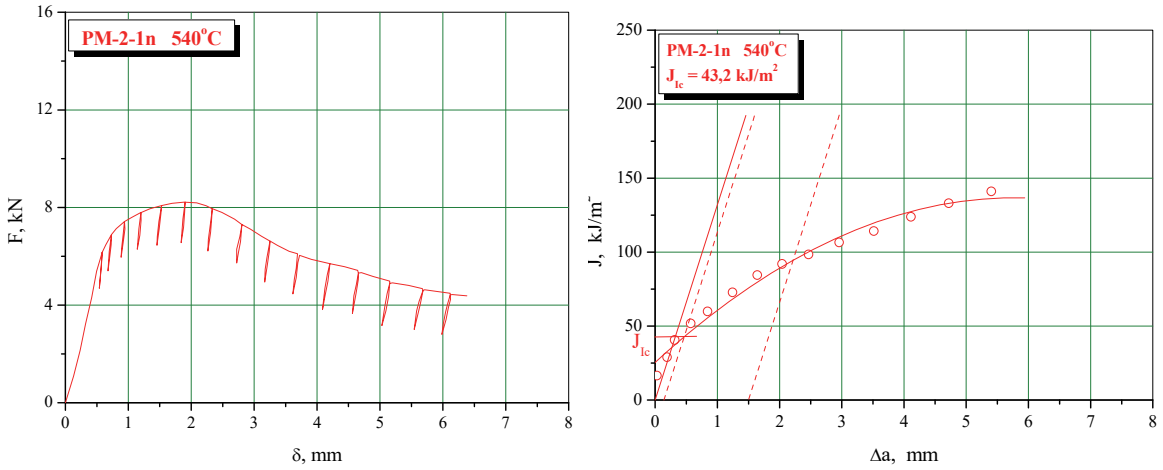

Figure 7: F-δ (left) and J-Δa (right) diagrams of specimen PM-2-1n.

The influence of testing temperature on the value of critical stress intensity factor, K_{Ic}, for specimens taken from the new and exploited PM is graphically illustrated in Fig. 8 (left), and the impact of the testing temperature on the critical crack length, a_c, is graphically illustrated in Fig. 8 (right), [1].

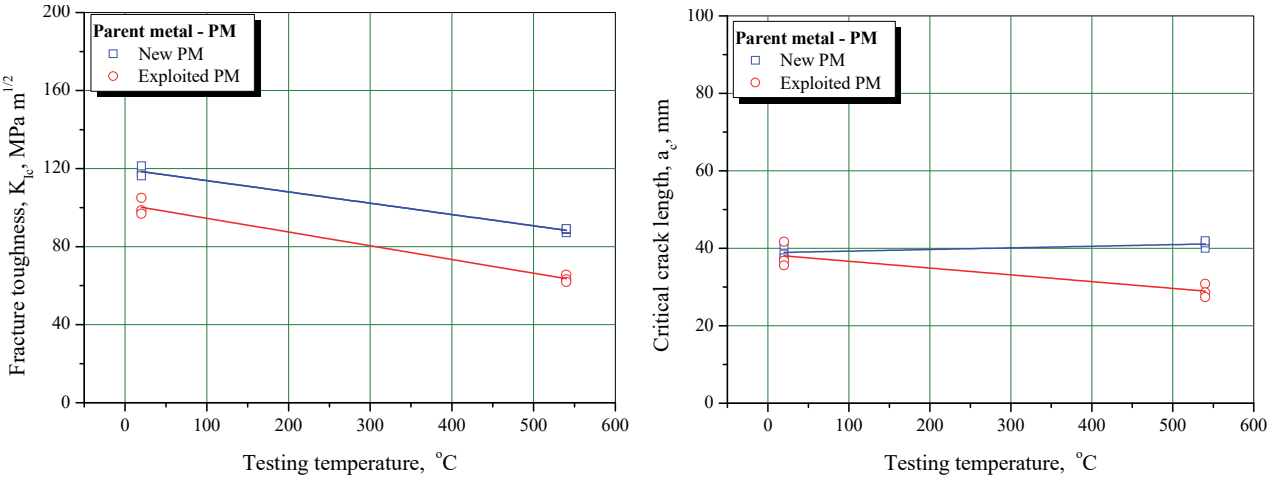

Figure 8: Changes in value of K_{Ic} depending on the testing temperature for the PM (left) and change in value of a_c (right)

Calculated values of critical stress intensity factor, K_{Ic}, and critical crack length, a_c, are given in the Tab.10 for notched specimens in WM, tested at room temperature of 20°C and working temperature of 540°C, [1].

Specimen mark	Testing temperature, °C	Critical J-integral, J_{Ic}, kJ/m²	Critical stress intensity factor, K_{Ic}, MPa m$^{1/2}$	Critical crack length, a_c, mm
WM-1-1		72.8	129.6	20.2
WM-1-2	20	74.3	130.9	20.7
WM-1-3		71.1	128.1	19.8
WM-2-1		50.2	93.9	17.4
WM-2-2	540	52.6	96.2	18.2
WM-2-3		48.4	92.2	16.8

Table 10: Values of, K_{Ic} notched specimens at WM.

Impact of the testing temperature on the value of critical stress intensity factor, K_{Ic}, for notched specimens in WM is graphically illustrated in Fig. 9 (left), and the impact of the testing temperature on the value of the critical crack length, a_c, is graphically illustrated in Fig. 9, (right) [1].

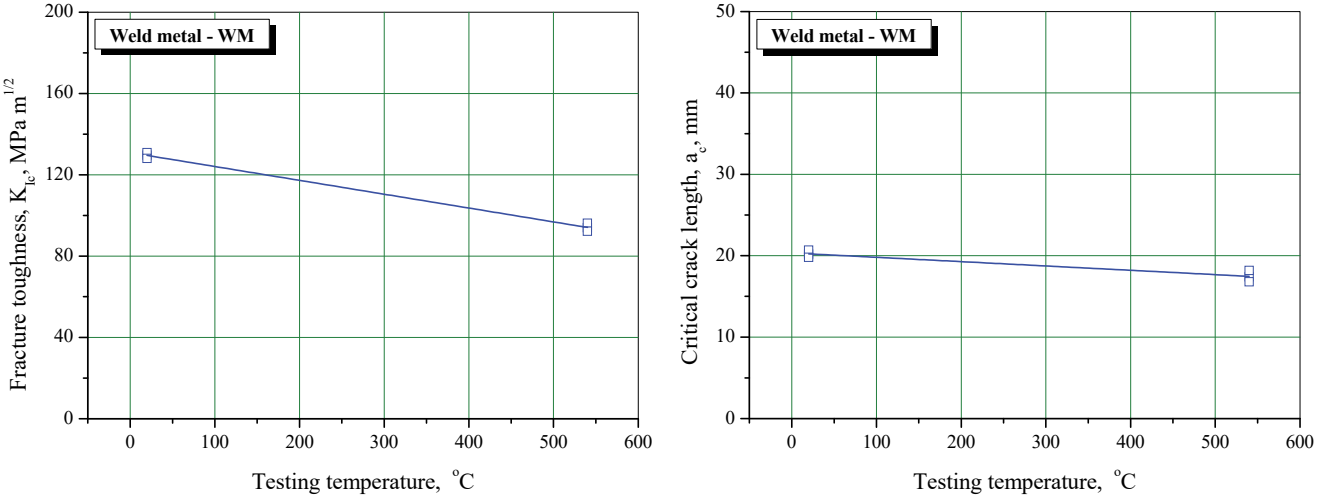

Figure 9: Changes in value of K_{Ic} depending on the testing temperature for the WM (left) and change in value of a_c (right).

Calculated values of critical stress intensity factor, K_{Ic}, and critical crack length, ac, are given in the Tab. 11 for notched specimens in HAZ from the side of the new PM and in Tab. 12 for notched specimens in HAZ from the side of the exploited PM, tested at room temperature of 20°C and working temperature of 540°C, [1].

Specimen mark	Testing temperature, °C	Critical J-integral, J_{Ic}, kJ/m²	Critical stress intensity factor, K_{Ic}, MPa m$^{1/2}$	Critical crack length, a_c, mm
HAZ-1-1n	20	53.6	111.2	34.3
HAZ-1-2n		51.7	109.2	33.0
HAZ-1-3n		49.8	107.2	31.8
HAZ-2-1n	540	33.6	76.9	31.1
HAZ-2-2n		34.2	77.5	31.6
HAZ-2-3n		36.1	79.7	33.4

Table 11: Values of, K_{Ic} notched specimens at new HAZ.

Specimen mark	Testing temperature, °C	Critical J-integral, J_{Ic}, kJ/m²	Critical stress intensity factor, K_{Ic}, MPa m$^{1/2}$	Critical crack length, a_c, mm
HAZ-1-1e	20	42.4	96.3	32.0
HAZ-1-2e		36.1	91.3	31.5
HAZ-1-3e		35.6	90.6	31.1
HAZ-2-1e	540	20.2	59.6	25.4
HAZ-2-2e		22.5	62.9	28.3
HAZ-2-3e		21.7	61.8	27.3

Table 12: Values of, K_{Ic} notched specimens at exploited HAZ.

Impact of the testing temperature on the value of critical stress intensity factor, KIc, for notched specimens in HAZ from the side of the new and exploited PM is graphically illustrated in Fig. 10 (left), and the impact of the testing temperature on the value of the critical crack length, ac, also for the notched specimens in HAZ from the side of the new and exploited PM is graphically illustrated in Fig. 10, (right) [1].

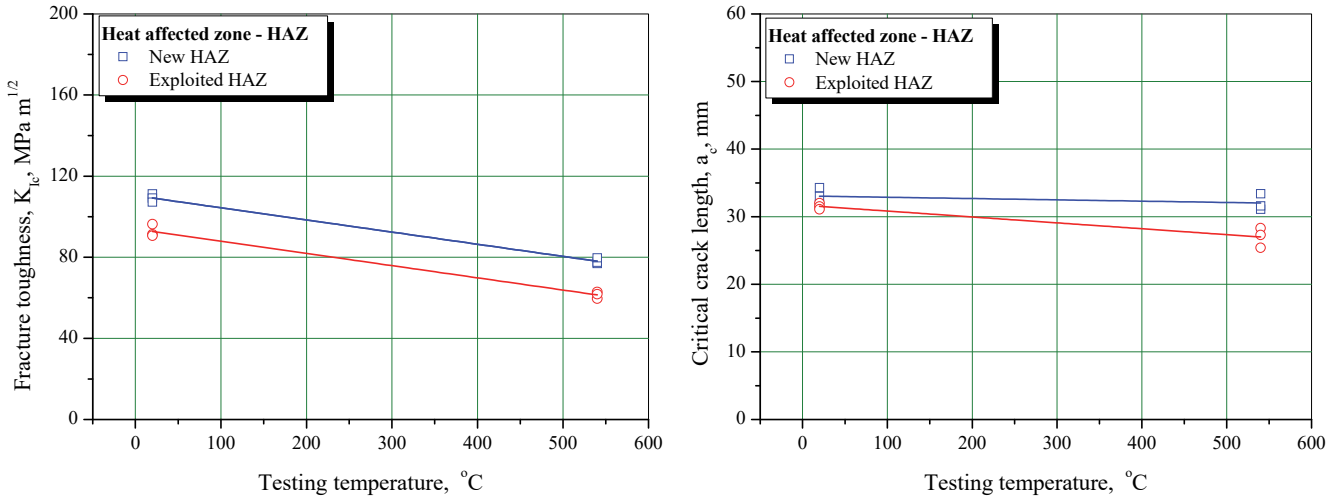

Figure 10: Change in value of K_{Ic} depending on the testing temperature at HAZ (left) and change in value of a_c (right).

Discussion

Testing of the welded joint specimens by introducing the load transversely to welded joint provided necessary data regarding how selected welding technology and exploitation time impact the welded joint strength and welded joint components. The obtained results of testing the welded joint specimens by introducing load transversely to welded joint, tab. 5, indicate that all tested specimens have cracked in exploited PM. This information is of great importance because it indicates the weakening of PM which was in exploitation. The fracture of specimens in PM clearly indicates the character of the welded joint. This is "over-matching", which means that the strength of the welded metal is higher than the strength of the parent metal, [1, 18]. Character of obtained tensile curves at room temperature corresponds to a ductile material with approximate share of homogeneous and non-homogeneous elongation at a ratio of 1/2:1/2. Here, homogeneous elongation is considered as elongation up to the maximum force, and non-homogenous elongation is considered as elongation from maximum force to fracture (unstable crack growth, i.e. necking). When testing the welded joint specimens at working temperature, there is a similar tendency of change in the properties of strength as with the testing at room temperature, but the difference occurs at the properties of strain (elongation). Namely, here we have the case where the ratio of homogeneous to non-homogeneous elongation is approximately 1/4:3/4, which is rather unfavourable from the aspect of exploitation properties. The reserve of homogenous plasticity of materials is considerably smaller, thus the hazard to PM of the consequences of potentially poor operation of the plant is real. By analysing the results obtained by tensile testing at room temperature of specimens taken from the sample of the new PM, given in tab. 6, it can be concluded that the testing results of the new PM are within the limits of values prescribed by the standard for that material, that is, values provided by a manufacturer in attest documentation. The obtained results of tensile testing of WM specimens given in tab. 7 confirm the properly selected welding technology, i.e. welding parameters. Yield stress and tensile strength satisfy values prescribed by the standard, whereas strain properties are much better than those given in the standard for this additional material, [19]. This phenomenon indicates a high-grade selected regime of thermal processing after welding. The behaviour of the HAZ in the loaded welded joint was conditioned by its small volume portion, as well as by the heterogeneity of the structure and different mechanical properties of certain HAZ areas. A well-made welded joint, designed according to the principle of higher WM strength, should break in PM, which is exactly what happened in presented tests, [1, 18].

Based on the obtained testing results of specimens taken from the new and exploited PM, WM and HAZ from the side of the new and exploited PM, it can be seen that with the increase of the testing temperature there is a decrease in the value of critical J_{Ic}, integral, that is, fracture toughness, KIc. The value of critical crack length, ac, also decreases.

The fracture toughness values, K_{Ic}, of specimens, taken from the new PM, tab. 8, range from 118MPa m1/2 obtained by testing at 20°C and decrease to 88MPa $m^{1/2}$ at 540°C. Also, the fracture toughness values, K_{Ic}, of specimens, taken from the exploited PM, tab. 9, range from 100MPa $m^{1/2}$ obtained by testing at 20°C and decrease to 64MPa $m^{1/2}$ at 540°C. The fracture toughness values, K_{Ic}, of specimens, taken from WM, tab. 10, range from 130MPa $m^{1/2}$ obtained by testing at 20°C to 94MPa $m^{1/2}$ obtained by testing at 540°C. The fracture toughness values, K_{Ic}, of specimens, taken from HAZ from the side of the new PM, tab. 11, range from 109MPa m1/2 obtained by testing at 20°C and decrease to 78MPa $m^{1/2}$ obtained by testing at 540°C. The testing of specimens taken from HAZ from the side of exploited PM, tab. 12, the poorer values of fracture toughness K_{Ic} are obtained. Namely, Namely, the value of plane strain fracture toughness, K_{Ic}, ranges from 93MPa $m^{1/2}$ obtained by testing at 20°C, and decreases to 61MPa $m^{1/2}$ obtained by testing at 540°C, [1].
The obtained values of critical crack length, a_c, fig. 10, at new PM are almost unchanged when it comes to room and working temperature. This was to be expected, because for the calculation of critical crack length, ac, the real values of yield stress obtained by tensile testing were used. However, exploitation weakening of PM has led to the fact that value of ac at specimens taken from exploited PM decreases by about 24% and is about 29mm.
The obtained values of critical crack length, a_c, fig. 12, at WM in relation to the yield stress level are quite low, and range from 20,2mm for the room temperature and decrease to 17,5mm which is the obtained value of a_c, at the testing temperature of 540°C. However, if values of critical crack length, a_c, in relation to yield stress of the new and exploited OM are calculated, they are significantly higher and indicate the good resistance to brittle fracture of WM.
The obtained values of critical crack length, a_c, fig. 14, at HAZ from the side of the new PM are slightly changed when it comes to room or working temperature. However, exploitation weakening of PM has led to the decrease of the value, a_c, at notched specimens in HAZ from the side of exploited PM and at the testing temperature of 5400C is 27mm, [1].

CONCLUSION

Based on the testing results of tensile properties of specimens taken from the welded joint of the new PM and WM at selected temperatures, it can be concluded that a decrease in strength properties, that is, yield stress and tensile strength was obtained with the increase of temperature. Likewise, the increase of testing temperature leads to the increase of elongation. The increase of elongation with the temperature increase is explained by the increased overall plasticity of the material at higher temperatures, but also by the significantly unfavorable ratio of homogenous and non-homogenous elongation. Also, the exploitation time significantly impacts the reduction of strength properties and strain properties, which can be related to the microstructures of the exploited and new PM, [1].
Based on the obtained testing results of the critical stress intensity factor K_{Ic}, which was due to inability to satisfy the plane strain conditions determined indirectly through the critical J_{Ic} integral, we can see that the values of K_{Ic} also depend on the testing temperature, placement of notches and exploitation time. The heterogeneity of welded joint mechanical properties, i.e. welded joint components significantly impacts the obtained values of plain strain fracture toughness, KIc.
The weakest resistance to the crack propagation at static action of force, that is, the lowest value, K_{Ic}, is at notched specimens in HAZ, and the best resistance to crack propagation is at notched specimens at WM. The character of the curves, exclusively changes depending on the testing temperature, placement of the notches and exploitation time. By analyzing the obtained curves, we see the almost identical character dependence of the individual curves in each group, except that the difference between the specimens is in the values of maximum force, Fmax, which is in direct dependence on the fatigue crack length, a, [1].
Exploitation time significantly impacted the resistance to crack propagation, which generally should be related to the weakening of mechanical exploitation properties of the used material in relation to the new material. The resistance to crack propagation, at specimens taken from the exploited PM and from HAZ from the side of exploited PM is for approximately 20% lower than at specimens taken from the sample of the new PM, and HAZ from the side of the new PM.
The obtained testing results of fracture mechanics parameters (K_{Ic}, J_{Ic} i a_c) indicate two things. First, tendency to brittle fracture in the conditions of static load acting, is the lowest at the notched specimens in WM and PM and is the highest at the notched specimens in HAZ, i.e. HAZ in the concrete case has the worst resistance to brittle fracture. Second, the obtained testing results of exploited material indicate a significant difference in the results compared to the new material.
Testing results and their analysis have justified the selected welding technology for the replacement of a part of the reactor mantle.

ACKNOWLEDGEMENT

Parts of this research were supported by the Ministry of Sciences and Technology of Republic of Serbia through Mathematical Institute SANU Belgrade Grant OI 174001 Dynamics of hybrid systems with complex structures. Mechanics of materials and Faculty of Technical Sciences University of Pristina residing in Kosovska Mitrovica.

REFERENCES

[1] Čamagić, I. (2013). Investigation of the effects of exploitation conditions on the structural life and integrity assessment of pressure vessels for high temperatures (in Serbian), doctoral thesis, Faculty of Technical Sciences, Kosovska Mitrovica.
[2] SRPS EN ISO 15614-1:2017, Specification and qualification of welding procedures for metallic materials - Welding procedure test - Part 1: Arc and gas welding of steels and arc welding of nickel and nickel alloys (ISO 15614-1:2017, Corrected version 2017-10-01), 2017.
[3] Burzić, M., (2008). Analiza parametara prsline toplo–otpornog čelika, Integritet i vek konstrukcija, 6(1), pp. 45-56.
[4] Čamagić, I., Sedmak, S., Sedmak, A., Burzić, Z. and Todić, A. (2017). Impact of Temperature and Exploitation Time on Plane Strain Fracture Toughness, K_{Ic}, in a Welded Joint, Structural Integrity And Life, 17(3), pp. 239–244.
[5] SRPS EN 895:2008, Destructive tests on welds in metallic materials - Transverse tensile test, (2008).
[6] SRPS EN 10002-1, Metallic materials - Tensile testing - Part 1: Method of test (at ambient temperature), (1996).
[7] SRPS EN 10002-5, Metallic materials - Tensile testing - Part 5: Method of testing at elevated temperature, (1997).
[8] ASTM E399-89, Standard Test Method for Plane-Strain Fracture Toughness of Metallic Materials, Annual Book of ASTM Standards, 03.01, pp. 522, (1986).
[9] ASTM E 1820-99a, Standard Test Method for Measurement of Fracture Toughness, Annual Book of ASTM Standards, 03.01, (1999).
[10] BS 7448-Part 1, Fracture mechanics toughness tests-Method for determination of KIc critical CTOD and critical J values of metallic materials, BSI, (1991).
[11] ASTM E813-89, Standard Test Method for J_{Ic}, A Measure of Fracture Toughness, Annual Book of ASTM Standards, 03.01, pp. 651, (1993).
[12] ASTM E 1737-96, Standard Test Method for J Integral Characterization of Fracture Toughness, Annual Book of ASTM Standards, 03.01, (1996).
[13] BS 7448-Part 2, Fracture mechanics toughness tests - Methods for determination of KIc, critical CTOD and critical J values of welds in metallic materials, BBI, (1997).
[14] ESIS Procedure for Determining the Fracture Behavior of Materials, European Structural Integrity Society ESIS P2-92, (1992).
[15] BS 5762-DD 19, Standard Test Method for Crack Opening Displacement, London, (1976).
[16] ASTM E1152-91, Standard Test Method for Determining J-R Curve, Annual Book of ASTM Standards, 03.01, pp. 724, (1995).
[17] ASTM E 1290-89, Standard Test Method for Crack-Tip Opening Displacement (CTOD) Fracture Toughness Measurement, Annual Book of ASTM Standards, 03.01, (1993).
[18] Camagic, I., Burzic, Z., Sedmak, A., Dascau, H. and Milovic, L. (2015). Temperature effect on a low-alloyed steel welded joints tensile properties, The 3rd IIW South – East European Welding Congress, Welding & Joining Technologies for a Sustainable Development & Environment, Timisoara, Romania, (77-81).
[19] Burzić, Z. (2002). Savremene metode provere mehaničko-tehnoloških osobina zavarenih spojeva-Deo 2, Zavarivanje i zavarene konstrukcije, 47(3), pp. 151-158.